Fracture Mechanics of Ceramics 13

Crack-Microstructure Interaction, R-Curve Behavior, Environmental Effects in Fracture, and Standardization

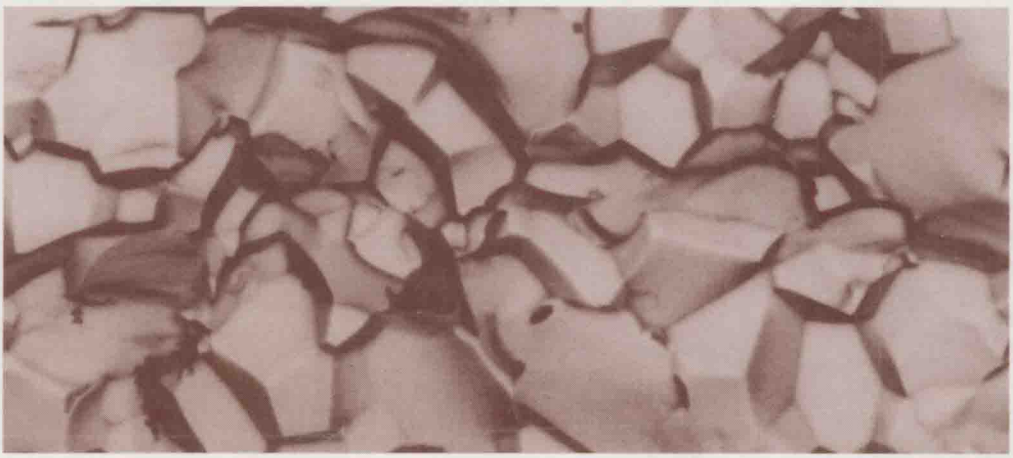

R. C. Bradt, D. Munz, M. Sakai,
V. Ya. Shevchenko, and K. W. White

Fracture Mechanics of Ceramics

Volume 13

Crack–Microstructure Interaction, R-Curve Behavior, Environmental Effects in Fracture, and Standardization

Edited by

R. C. Bradt
University of Alabama
Tuscaloosa, Alabama

D. Munz
University of Karlsruhe
Karlsruhe, Germany

M. Sakai
Toyohashi University of Technology
Toyohashi, Japan

V. Ya. Shevchenko
Institute of Silicates Chemistry
RAS, St. Petersburg, Russia

and

K. White
University of Houston
Houston, Texas

Kluwer Academic/Plenum Publishers
New York, Boston, Dordrecht, London, Moscow

Proceedings of the 7th International Symposium on the Fracture Mechanics of Ceramics, held July 20–22, 1999, in Moscow, Russia

ISBN 0-306-46663-5

233 Spring Street, New York, N.Y. 10013

http://www.wkap.nl

10 9 8 7 6 5 4 3 2 1

A C.I.P. record for this book is available from the Library of Congress

Printed in the United States of America

Fracture Mechanics of Ceramics

Volume 13

Crack–Microstructure Interaction, R-Curve Behavior, Environmental Effects in Fracture, and Standardization

Volume 1	Concepts, Flaws, and Fractography
Volume 2	Microstructure, Materials, and Applications
Volume 3	Flaws and Testing
Volume 4	Crack Growth and Microstructure
Volume 5	Surface Flaws, Statistics, and Microcracking
Volume 6	Measurements, Transformations, and High-Temperature Fracture
Volume 7	Composites, Impact, Statistics, and High-Temperature Phenomena
Volume 8	Microstructure, Methods, Design, and Fatigue
Volume 9	Composites, R-Curve Behavior, and Fatigue
Volume 10	Fracture Fundamentals, High-Temperature Deformation, Damage, and Design
Volume 11	R-Curve Behavior, Toughness Determination, and Thermal Shock
Volume 12	Fatigue, Composites, and High-Temperature Behavior
Volume 13	Crack–Microstructure Interaction, R-Curve Behavior, Environmental Effects in Fracture, and Standardization

PREFACE

This Volume 13 of the Fracture Mechanics of Ceramics series constitutes the Proceedings of the 7th International Symposium on the fracture mechanics of ceramics held at the Presidium of the Russian Academy of Sciences, Moscow, Russia on July 20 to 22, 1999. The series started from the Proceedings of the 1st Symposium at the Pennsylvania State University that has been held on 1973 (Vols. 1 and 2), followed by 1977 and 1981 Years meetings (Vols. 3 to 6) which were held at the Pennsylvania State University, too. Volumes 7 and 8 are from the 1985 Symposium which was held at the Virginia Polytechnic Institute and State University, Volumes 9 and 10 are from the 1991 Symposium at Japan Fine Ceramic Centre, Nagoya, and Volumes 11 and 12 are from the 1995 Symposium at Kernforschungszentrum, Karlsruhe.

The theme of the Symposium was focused on the mechanical behaviour of advanced ceramics in terms of the cracks, particularly the crack-microstructure interaction, delayed failure, environmental effects in fracture. Special attention was paid on the novel methods in fracture mechanics testing, pre-standardisation and standartisation. The authors from 19 countries represented the current state of that field.

The International Scientific Committee gratefully acknowledge the sponsoring provided by The Russian Academy of Sciences and, personally, Academician Yu.S.Osipov, President of RAS; The Ministry of Science and Technologies of the Russian Federation, Prof. G.Terestchenko; Russian Foundation for Basic Research, Academician I.Moiseev; Scientific Technical Center "Bacor", Dr. B.Krasnij; Gzhel Ltd., Prof. V.Loginov, I.Leitis, and Adamant Ltd. Without their support, the magnitude and quality of this meeting simply would not have been possible.

The International Scientific Committee would like to thank the members of the Local Organizing Committee for efficient organization and, especially, Prof. S.Barinov, Eng. Yu.Tutkova and Eng. N.Fomina for their help in the preparation of the manuscript.

R.C.Bradt
Tuscaloosa, USA

D.Munz
Karlsruhe, Germany

M.Sakai
Toyohashi, Japan

V.Ja.Shevchenko
Moscow, Russia

K.White
Houston, USA

CONTENTS

CALCULATION OF CRACK TIP PHASE TRANSFORMATION ZONES IN TZP WITH THE WEIGHT FUNCTION METHOD

G. Rauchs[1], D. Munz[2], T. Fett[2]

[1]Materials Science Centre, University of Manchester, Grosvenor Street, Manchester M1 7HS, U.K.
[2]Forschungszentrum Karlsruhe, Institut für Materialforschung II, and Universität Karlsruhe, Institut für Zuverlässigkeit und Schadenskunde im Maschinenbau, PF 3640, D-76021 Karlsruhe, Germany

Key words: Ce-stabilized zirconia, Phase transformation zones, Weight function technique.

ABSTRACT

Stabilized zirconia ceramics can undergo a stress-induced tetragonal-to-monoclinic phase transformation. This way, a transformation zone with compressive stresses develops around crack tips, leading to an increase in fracture toughness. The increase in fracture toughness depends on the size of the transformation zone. Therefore, the ability to compute the phase transformation zone at a crack tip is crucial to determine the transformation toughening due to phase transformation. In the case of subcritical phase transformation, the crack tip phase transformation zone has been calculated using the finite element method. In some zirconia ceramics, like ceria-stabilized TZP zirconia ceramics, an autocatalytic phase transformation takes place, leading to large, elongated transformation zones. As this supercritical phase transformation cannot be computed with finite elements, several methods for investigating supercritical phase transformation have been developed. In this paper, a method based on the weight function method will be described.

1. INTRODUCTION

Stabilized zirconia ceramic materials exhibit a fracture toughness ranging well above fracture toughnesses observed in other common ceramic materials like Al_2O_3, SiC or Si_3N_4. The high toughness in zirconia is due to transformation toughening: in this material, a stress-induced tetragonal-to-monoclinic phase transformation takes place. Therefore, a transformation zone develops at the crack tip of a loaded crack, which leads to a layer of compressive stresses around the crack tip, reducing the load at the crack tip. Since the amount of transformation-induced crack-tip shielding is related to the size of the

Fracture Mechanics of Ceramics, Vol. 13
Edited by R.C. Bradt *et al.*, Kluwer Academic/Plenum Publishers, 2002

transformation zone and to the height of the transformation zone in the case of crack growth, the amount of crack-tip shielding can be predicted if the geometry of the transformation zone can be calculated. In a simple approach, the crack tip stress field, for which analytical solutions are known, can be introduced into a multiaxial transformation criterion, which yields the transformation zone for the case of weak transformation, i.e. the influence of the transformation strains on the crack tip stress field is neglected.

Due to the singular stress field near a crack tip in transformation-toughened zirconia, the material undergoes a stress-induced martensitic transformation and the tetragonal phase changes to the monoclinic phase (t- to m-ZrO_2). This transformation occurs when the local stresses reach a critical value and the result is a crack-tip transformation zone. In early studies it was assumed by McMeeking and Evans [1] that the transformation is initiated when the hydrostatic tensile stress reaches a characteristic value $\sigma_{hyd,c}$. For the special case of small-scale transformation conditions (transformation zone size negligible compared with crack size and component dimensions) McMeeking and Evans [1] and Budiansky et al. [2] computed the transformation zone, neglecting the perturbation of the stress field due to transformations. For the special case of phase transformation activated by hydrostatic stress, the size and shape of the zone results from the condition that the hydrostatic stress σ_{hyd} equals a critical value $\sigma_{hyd,c}$.

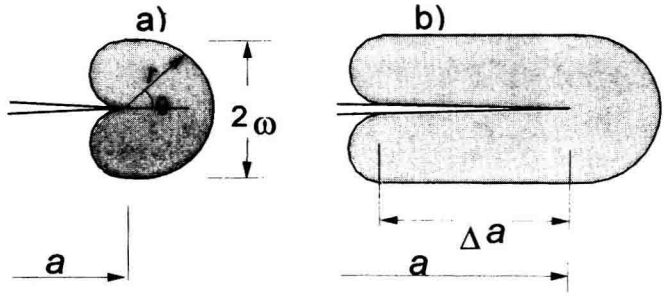

Figure 1. Zone ahead of a crack tip: a) without crack propagation, b) after crack extension.

In this case the phase transformation zone for plane strain becomes

$$\omega = \frac{(1+\nu)^2}{4\sqrt{3}\,\pi}\left(\frac{K_I}{\sigma_{hyd,c}}\right)^2, \quad r = \frac{8}{3\sqrt{3}}\omega\cos^2(\theta/2) \tag{1}$$

Figure 1 illustrates the transformation zone for a non-extending crack (a) and after a crack extension of Δa (b). Caused by the martensitic transformation, a volumetric expansion strain of about 4.5% occurs. These strains cause tensile stresses at some distance ahead of the crack tip and compressive stresses along the length Δa at the crack line. The compressive stresses lead to a shielding stress intensity factor which has to be overcome during crack propagation, i.e. the applied stress intensity factor must be increased to maintain stable crack growth.

For the computation of more realistic shielding stress intensity factors, the change of the transformation zone due to the transformation stresses has to be taken into consideration ("strong" phase transformation). Such computations using the finite element method have been achieved by [2][3] for the hydrostatic transformation criterion and by [4] for a shear-dilatant transformation criterion. In both cases, solutions have been presented. In the case of supercritical phase transformation, with a burst-like, discontinuous transition from the

tetragonal to the monoclinic phase, the loss of ellipticity of the governing differential equations inhibits the use of the finite element method.

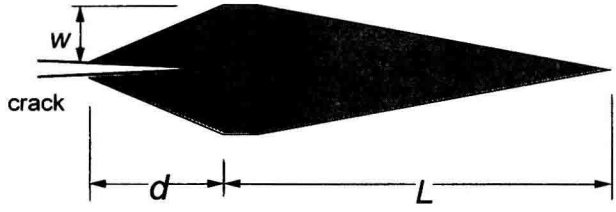

Figure 2. Shape of phase transformation zones in ceria-partially-stabilized zirconia.

For the nearly circular phase transformation zones which are found in MgO-doped zirconia, an increase of the crack growth resistance to a maximum value within a small amount of crack extension is expected. In contrast, the zone shape of Ce-partially stabilized zirconia differs strongly. Figure 2 illustrates a typical elongated transformation zone as reported by Yu et al. [5]. It was experimentally found that the shape of the deformation zone, characterized by w/L and w/d, changes with crack extension. The shielding stress intensity factor K_s can be expressed as [5]

$$K_s = \left\{ \frac{\varepsilon^T E f}{1-\nu} \left[\sqrt{\frac{w}{d}}\, \kappa\left(\frac{w}{d}, \frac{w}{L}\right) \right] \right\} \sqrt{d_0 + \Delta a} \qquad (2)$$

(with $d_0 = d$ for $\Delta a = 0$), where the function $\kappa(w/d, w/L)$ was calculated applying the weight function method. In Figure 3 the experimentally observed R-curve is plotted together with the computed stress intensity factors shown as the shaded area. The scatter in the computations results from the scatter in the transformation zone shape. It can be seen that for elongated transformation zones the R-curve increases within a large amount of crack extension.

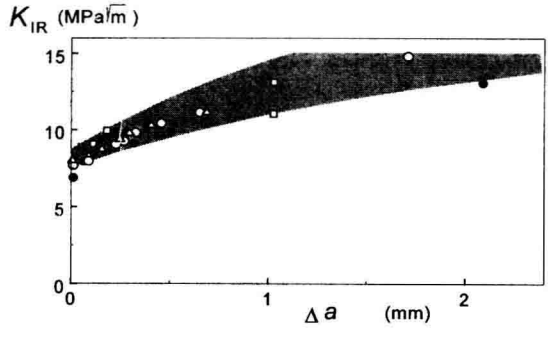

Figure 3. Comparison of measured R-curve data (symbols) and computed stress intensity factors (shaded area) according to Yu et al. [5].

As mentioned before the R-curve computations in [5] were based on the experimentally observed zone sizes. The remaining question is, why the transformation zones have the observed shape.

Efforts have been made to treat the supercritical phase transformation like a shock wave propagation. Using a finite difference code, crack tip transformation zones have been calculated for out-of-plane loads by [6]. In another approach, the crack tip transformation zone has been modelled by considering a multitude of independent transformable circular inclusions around a crack tip by [7]. In the following sections, a kinematic, semi-analytical iterative computing scheme to calculate the crack tip transformation zone is being presented. In this approach, the stress field of a transformed inclusion at a crack tip is considered as the linear superposition of three stress fields:

- the stress field of the crack loaded with an external load
- the stress field caused by the transformation strains in the vicinity of the crack tip
- the stress field produced by the transformation strains in the absence of a crack

For the first stress field, analytical solutions are known. The last two stress fields have to be calculated using the weight function method for the former and Eshelby's method for the latter case. To simplify the calculations, only cases symmetrical to the crack plane are considered.

2. CALCULATION OF THE TRANSFORMATION STRAIN RELATED STRESS FIELDS

The crack tip transformation zone is considered a transformed inclusion which has undergone unconstrained transformation strains ε^{T}_{ij}, known from the difference of the lattice parameters of the monoclinic and tetragonal phases. In order to make the transformation strains accessible for further computations, the transformation strains inside of the inclusion, assumed to be constant, are transformed into tractions at its boundary using the strain suppression method of [8]. This method consists of four different virtual steps:

a) the untransformed transformation zone is cut free from the continuum (Figure 4a)
b) the transformation zone undergoes an unconstrained transformation strain ε^{T}_{ij} (Figure 4b)
c) tractions $-t_j$ are applied along the zone boundary to restore the inclusion to its original shape (Figure 4c). The tractions t_j are calculated with the normal n_i using Hooke's law:

$$t_j = n_j \varepsilon^{T}_{ij} = \frac{E\nu}{(1+\nu)(1-2\nu)} \varepsilon^{T}_{mm} n_j + \frac{E}{1+\nu} \varepsilon^{T}_{ij} n_i \qquad (3)$$

d) the transformation zone is reinserted into the continuum and welded to it. Furthermore, tractions t_j of opposite sign are applied to the zone boundary to restore equilibrium (Figure 1d).

In the case of an incomplete phase transformation, the tractions are multiplied by a scalar f with $0 < f < 1$ equal to the true monoclinic phase content. For reasons of simplicity it is assumed that the elastic constants of both parent and product phase are identical.

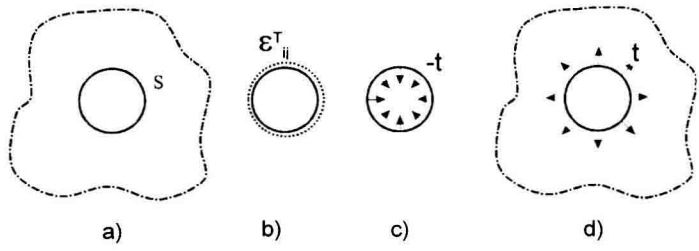

Figure 4. The strain suppression method of Eshelby.

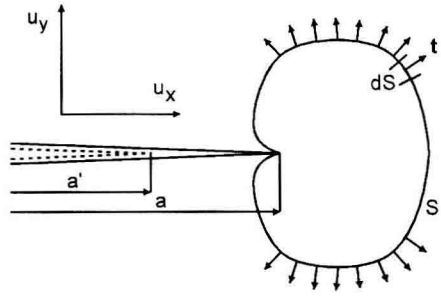

Figure 5. Loaded transformation zone boundary at the crack tip.

The stress field caused by the interaction of transformation strains with the crack tip can be calculated using the weight function method. With symmetry being assumed, only mode-I stress intensity factors have to be considered. The stress intensity factor produced by tractions t_j along a curve (Figure 5) can be computed as:

$$K = \oint_S t_i h_i \, dS \tag{4}$$

with the weight function h_i defined by a reference stress intensity factor K_r, the elastic constants E and ν, the displacement u_i and the crack length a as:

$$h_i = \frac{E}{1-\nu^2} \frac{1}{K_r} \frac{\partial u_i}{\partial a} \tag{5}$$

In order to perform simple numerical computations, where the zone size is assumed to be small compared with the crack length and with the component dimensions, the near-tip weight function [1] can be applied:

$$h_x = \frac{1}{\sqrt{8\pi(1-\nu)}} [2\nu - 1 + \sin(\theta/2)\sin(3\theta/2)]\cos(\theta/2) \tag{6}$$

$$h_y = \frac{1}{\sqrt{8\pi(1-\nu)}} [2 - 2\nu - \cos(\theta/2)\cos(3\theta/2)]\sin(\theta/2) \tag{7}$$

Equation (5) can be transformed into an integral equation yielding the displacement field around the crack tip [9]:

$$u_i = \frac{1-\nu^2}{E}\int_0^a K_r(a')\,h(a')\,da' + u_{i0} \tag{8}$$

In order to solve eq.(8), a large number of reference load cases for virtual crack lenghts a' as shown in Figure 5 have to be evaluated using eq.(4). Inserting eq. (4) into eq.(8) yields the displacement field caused by the transformation strains:

$$u_i = \frac{1-\nu^2}{E}\int_0^a \oint h_i t_i \, dS \cdot h(a')\,da' + u_{i0} \tag{9}$$

The integration constant u_{i0} of eq.(9) is the displacement field produced by the transformation strains in the absence of a crack. This displacement field can be computed by integrating the tractions with the Kelvin solutions U_{ij} along the transformation zone boundary [8]:

$$u_{i0} = \oint_S U_{ij} t_j \, dS \tag{10}$$

By differentiation, the elastic strains are derived from the displacements:

$$\varepsilon_{ij} = \tfrac{1}{2}(u_{i,j} + u_{j,i}) \tag{11}$$

Using Hooke's law, the stresses can be calculated:

$$\sigma_{ij} = \frac{E\nu}{(1+\nu)(1-2\nu)}\varepsilon_{mm} + \frac{E}{1+\nu}\varepsilon_{ij} \tag{12}$$

For calculating the crack tip transformation zone including the effect of transformation strains, the transformation zone for weak phase transformation is computed first by inserting the stress field caused by the external load of the crack into a multiaxial transformation criterion. Then, the following steps are performed:

a) the transformation zone boundary is discretised at a number of boundary points.
b) the stress fields due to transformation strains are calculated at the boundary points and at several interpolation points normal to each boundary point using eqs.(9-12).
c) the global stress field resulting from the superposition of the stress field of the external load and those calculated before are introduced into the transformation criterion, yielding a new transformation zone boundary.

Steps a) through c) are iteratively repeated until a converging zone boundary is found.

3. RESULTS

This computing scheme mentioned before has been used with the hydrostatic transformation criterion by [9]. Performing computations for the maximum principal stress criterion with parameters obtained in experiments [10], i.e. a critical transformation stress $\sigma^*_{1,c}$ = 300 MPa and a monoclinic phase content f = 40%, no convergence of the zone boundary was found. This is due to the large stresses arising from the displacement field u_{i0}, which does not contribute to the global hydrostatic stress field, i.e. $\sigma_{h0} = 0$, but produces a strong stress concentration at the zone boundary which inhibits the zone boundary convergence for the transformation criterion considered.

Accordingly, in order to assess the influence of the transformation strains on the transformation zone boundary, computations have been performed using a monoclinic phase content f ranging from 5 to 20 % for finding converging transformation zones. Figure 6 shows the upper half of the transformation zone found for a monoclinic phase content f = 10%. It is obvious that the transformation zone shape strongly differs from the weak phase transformation solution. With the transformation strains included in the calculations, a strongly elongated zone shape is found. The transformation zone height is related to the weak phase transformation solution, whereas it was found that the elongation of the zone increases with increasing monoclinic phase content.

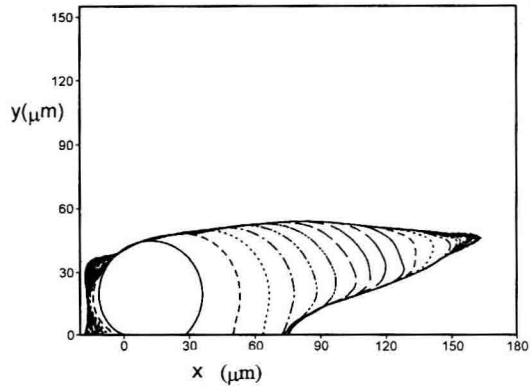

Figure 6. Iterative solutions of the transformation zone at a crack tip for a critical normal stress of 300 MPa and a reduced monoclinic phase content of 10%.

Similar results with a strongly elongated transformation zone have been found for the shear-dilatant criterion derived in [11]. A comparison of the calculated crack tip transformation zones with experimentally observed transformation zones on ceria-stabilized zirconia SEVNB-specimens shows a good agreement as far as the elongated transformation zone shape is concerned. The irregular, dendritic shape cannot be predicted with the calculating scheme. Nevertheless, it was found that small oscillations in the discretisation of the zone boundary are strongly enhanced throughout the iterative computing process. This seems to be a feature of the stress field caused by the supercritical phase transformation and might explain the development of a strongly irregular transformation zone in the real material (Figure 7), where a disturbed transformation zone boundary is to be expected due to microscopic inhomogeneities.

4. CONCLUSIONS

The semi-analytical, iterative method developed in this paper enables the calculation of crack tip transformation zones with the effect of the transformation strains on the crack tip stress field for the case of supercritical phase transformation being included using the weight function method and Eshelby's method. It was shown that the transformation strains produce an elongated transformation zone which strongly differs from the transformation zones computed when neglecting the transformation strains. The shape of the calculated transformation zones is in good agreement with experimentally observed, elongated transformation zones found on the SEVNB specimen of supercritically transforming zirconia ceramics.